

Received: 2015.06.19
Accepted: 2015.09.09
Published: 2016.02.27

Relationship Between P15 Gene Mutation and Formation and Metastasis of Malignant Osteosarcoma

Authors' Contribution:
Study Design A
Data Collection B
Statistical Analysis C
Data Interpretation D
Manuscript Preparation E
Literature Search F
Funds Collection G

EFG **ChangShui Yu**
ABCD **WenBo Wang**

Department of Orthopedics, The First Affiliated Hospital of Harbin Medical University, Harbin, Heilongjiang, P.R. China

Corresponding Author: Wenbo Wang, e-mail: minebs77hii@yeah.net
Source of support: Departmental sources

Background: As a type of primary malignant bone tumor, osteosarcoma has high incidence and poor prognosis, and is predisposed for pulmonary metastasis. The abnormal expression of P15 gene directly participates in the invasion of various cancers. Therefore, this study investigated the gene mutation of P15 in both primary lesion and pulmonary metastasis lesion of osteosarcoma in a rat model, in an attempt to elucidate the value of P15 gene as a biological marker.

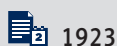
Material/Methods: A total of 60 SD rats were randomly divided into 2 groups. Model rats had injection of osteosarcoma UMR-106 cells (5×10^6) inoculated underneath the right forelimb skin, while control rats received saline injection instead. Six rats were sacrificed after 0, 1, 2, 4, and 6 weeks of the inoculation. Tissue samples from inoculation sites and lungs were extracted for measuring the tumor size. SP immunohistochemical (IHC) staining was used to detect the positive expression rate, while P15 gene mutation was detected by PCR method.

Results: With the elongation of inoculation time, tumor size was significantly increased ($p < 0.05$). The positive expression rates in both primary and pulmonary metastasis lesions were also significantly elevated ($p < 0.05$). The occurrence rate of P15 gene mutation in model rats was significantly elevated and showed a correlation with the tumor formation ($r = 0.998$, $p < 0.05$).

Conclusions: The P15 gene mutation was significantly correlated with osteosarcoma formation and metastasis towards the pulmonary tissue, suggesting its potency as a novel biological marker for early diagnosis of osteosarcoma.

MeSH Keywords: **Imaging, Three-Dimensional • NM23 Nucleoside Diphosphate Kinases • Transcription Factor TFIIIA**

Full-text PDF: <http://www.medscimonit.com/abstract/index/idArt/895022>



1923



3



2



25



Background

Osteosarcoma is a common primary malignant bone tumor with complicated pathogenesis and frequent distal metastasis, thus causing higher mortality rates, especially in the teenagers [1]. Epidemiological surveys revealed that nearly 40% of osteosarcoma patients died from misdiagnosis and/or early tumor metastasis, especially toward the lung tissue [2–4]. Therefore, it is of critical importance to find a simple and effective biological marker for osteosarcoma, in order to make early diagnosis. Current studies have revealed the role of gene mutation in the proliferation of tumor cells. Cell apoptosis-related genes, including vascular epithelial growth factor (VEGF) and microRNA (miR)-96, were found to be closely correlated with the occurrence and prognosis of osteosarcoma [5,6]. P15, a novel tumor-suppressor gene, has been reported to play an important regulatory role in the progression of various malignant tumors, such as pulmonary cancer, nasopharynx cancer, and kidney cancer [7]. The fragment loss, point mutation, or methylation of P15 gene may all lead to its abnormal tumor-suppressing function, thus facilitating the malignancy and metastasis of tumor cells [8]. Previous studies have been performed on the pathogenesis and related mechanisms of pulmonary metastasis of osteosarcoma [9], but the involvement of P15 gene has not been reported. As it is of critical importance for early diagnosis of osteosarcoma to discover a simple but effective biological tumor marker, this study aimed to describe the mechanism of P15 gene mutation in the occurrence and lung metastasis of osteosarcoma in a rat model, as previously described [10]. This study may provide further evidence for developing methods in clinical diagnosis of malignant osteosarcoma.

Material and Methods

Animal model

A total of 60 SD rats (both males and females, ages 4–5 weeks, body weight 150–170 g) from the Laboratory Animal Center of Harbin Medical University, were randomly divided into control and model groups (N=30 each). The osteosarcoma model was prepared as previously reported [11]. In brief, after general anesthesia, 0.5 mL UMR-106 cell suspensions (ATCC, US, 1×10^7 per mL), which were cultivated in DMEM containing 10% fetal bovine serum (GIBCO, USA), were subcutaneously injected into the right forelimb of each rat in the model group. Control rats received equal volumes of 0.9% saline instead.

Rats were used for all experiments, and all procedures were approved by the Animal Ethics Committee of Harbin Medical University.

SP-immunohistochemical (IHC) staining

After 0, 1, 2, 4, and 6 weeks of the inoculation, 5 rats from model or control groups were sacrificed to separate osteosarcoma and pulmonary tissues. Morphological changes were observed, along with the measurement of tumor size. The tumor volume was approximated as: (short diameter \times long diameter)²/2, as reported elsewhere [12]. The isolated pulmonary tissue was fixed in 10% neutral buffered formalin, followed by xylene dewaxing and gradient ethanol (100%, 95%, 80%, and 70%) hydration. We added 20 μ g/ml protease K without DNase to incubate at 37°C for 15 min, and then it was boiled in citric acid buffer (0.01M, pH =6.0) for 20 min after being washed 3 times (5 min each time) with PBS until naturally cooling down to room temperature. PBS containing 5% normal goat sera was used to block at 37 for 10 min, then the sera was decanted and added to primary antibody. The sample was at 4°C overnight. After being washed with PBS for 3 times, secondary antibody containing 1% labeled biotin was applied for incubation at 37°C for 15 min. After being washed with PBS for 3 times, 3% horseradish peroxidase-labeled avidin working solution was used for incubation at 37°C for 15 min. DAB staining was conducted after being washed with PBS 3 times, and then it was washed with tap water, following hematoxylin re-dyeing, drying, and mounting. The apoptotic cells were observed and photographed with an optical microscope. SP-IHC staining was used to show the positive expression of tumors cells and metastatic conditions. For a quantitative analysis, 10 randomly selected fields were counted for the percentage of tumor cells against total cells. A percentage higher than 50% was defined as positive expression. We carefully followed the instructions in the SP-IHC detection kit (Shanghai Yanhui Bio-tech, China).

PCR for P15 gene mutation

Peripheral blood samples (0.5 mL) were collected from all animals at the same time points, as detailed above. After centrifugation for 10 min at 3000 g, lower blood clots were lysed in PBS buffered-lysing reagents. Total RNA were then extracted from blood cells for further synthesis of cDNA, which was then used as the template in PCR assay for the analysis of 2nd exon of P15 gene.

Using specific designed primers (P15-F, 5'-TGGCT CTGAC CACTC TGC-3'; P15-R, 5'-AGCGA ATTCG GGTGG GAA-3') and internal reference gene β -actin (Forward, 5'-GAAAC TACGT TCAAG CGATC-3'; Reverse, 5'-CTAGA AGCAT TTGCG GTGGA-3'), PCR was performed in the following mixture: 1 μ L 10 \times reaction buffer, 70 μ M dNTPs (4 \times), 100 ng DNA templates, 30 ng primers, 100 ng Taq DNA polymerase, plus ddH₂O (up to 10 μ L). The reaction parameter was: pre-nature at 95°C for 5 min, followed by 40 repeating cycles each containing 95°C denature for 30 s,

Table 1. Tumor size and volume.

Group	Time after inoculation				
	0 week	1 week	2 weeks	4 weeks	6 weeks
Control (in mm ³)	0	0.15±0.03	0.32±0.05	0.24±0.08	0.15±0.04
Model (in mm ³)	0	4±0.18*	8±0.25*	17±0.23*	21±0.31*

* p<0.05 compared to the control group at the same time point.

Table 2. Tumor cells percentage by SP-IHC staining.

Group	N	Primary injection site					Pulmonary tissues				
		0 wk	1 wk	2 wks	4 wks	6 wks	0 wk	1 wk	2 wks	4 wks	6 wks
Model	25	13%	35%*	56%*	70%*	85%*	10%	24%*	51%*	63%*	72%*
Control	30	12%	17%	25%	32%	37%	8%	12%	23%	28%	34%

* p<0.05 compared to the control group at the same time point.

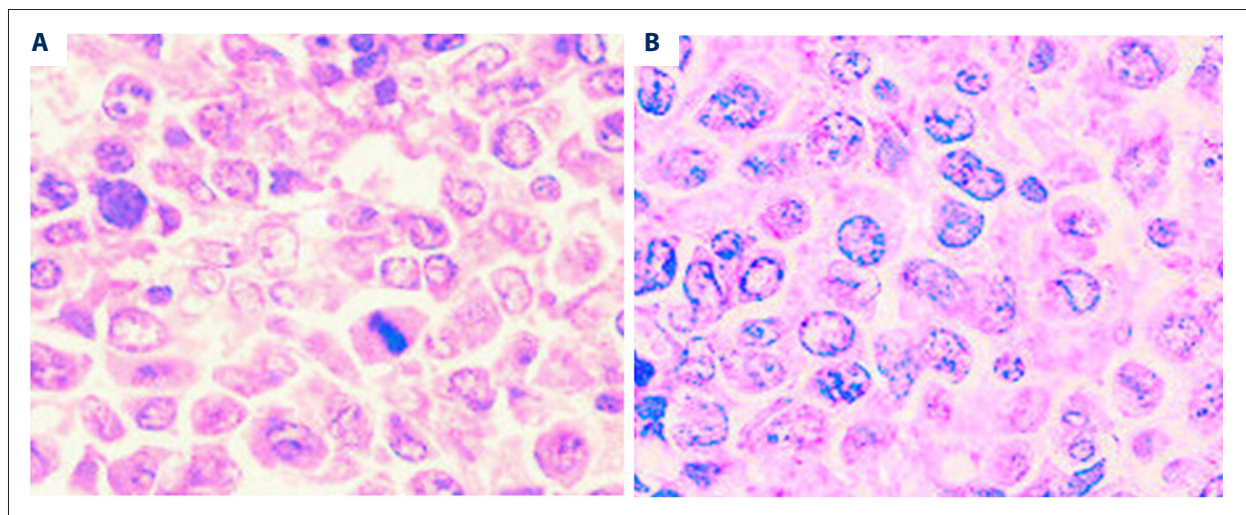


Figure 1. Images for SP-IHC staining (×200). (A) Cells from normal pulmonary tissues before inoculation, expression ratio from samples in model and control groups were 10% and 8%, respectively, and showed negative staining for tumor cells. (B) pulmonary tissues 6 weeks after injecting osteosarcoma cells. The expression ratio of tumor cells in the control group was 34%, indicating a negative value. However, abnormal nucleus/cytoplasm ratio, swelling of the nucleus, and deformity in lung tissues were found in the model group, in which the tumor cells tested positive with 72% of the expression ratio.

60°C annealing for 30 s, and 72°C elongation for 30 s. The reaction was ended by final elongation at 72°C for 8 min. Agarose gel (1%) electrophoresis was used to visualize PCR fragments lengths, along with β-actin-controlled fragments (232 bp).

Statistical analysis

SPSS 20.0 software package was used to analyze all collected data, which are presented as mean±standard deviation (SD). Between-group comparison was performed using analysis of variance (ANOVA). The correlation analysis was accomplished by Spearman test. A statistical significance was defined when p<0.05.

Results

Tumor size of osteosarcoma lesion

One week after the inoculation of tumor cells, there were small tumor lesions underneath the skin around the injection sites. As shown in Table 1, the average size of these tumors was 4.00±0.18 (in mm³). Abnormally enlarged microvessels can be observed on the surface and in the peripheral muscles of the tumor, even by the naked eye. On the second week, the tumor size increased to 4.00±0.25 (in mm³), with severe edema on the surface and in peripheral tissues. On the fourth

Table 3. P15 gene mutation and osteosarcoma formation.

Grup	N	Time after inoculation				
		0 week	1 week	2 weeks	4 weeks	6 weeks
Model	25	0	4.0%*	8.0%*	16.0%*	20.0%*
Control	30	0	0	3.3%	3.3%	6.7%

p<0.05 compared to the control group at the same time point.

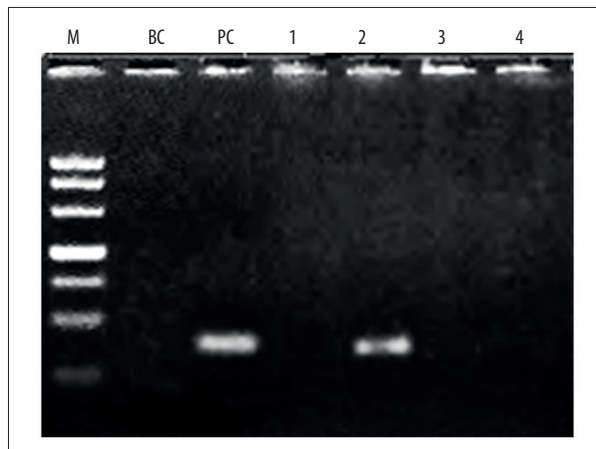


Figure 2. Electrophoresis of PCR products for P15 gene. M – DNA size marker; BC – blank control; PC – positive control; 1–4, different samples from the model group. Animals No. 1, 3, and 4 – had mutated P15 genes, while animal No. 2 – had wild-type gene.

and sixth weeks after injection, tumor size continued to grow (17.00 ± 0.23 and 21.00 ± 0.31 , in mm^3 respectively) but more slowly. A longitudinal dissection of the tumor revealed white and hard tissues with centralized necrosis.

Tumor cell percentage of osteosarcoma and pulmonary metastatic lesions by SP-IHC

Before tumor cell inoculation, negative staining results were obtained from all rats. After the injection of osteosarcoma cells, model rats had significantly elevated tumor cell percentage with the elongation of time. On the first week, most of osteosarcoma and pulmonary tissues showed negative staining for tumor cells. From week 2, positive staining cells began to occur in model rats but not in control rats. On week 6, the tumor positive rates were as high as 85% and 72% in primary and pulmonary tissues, respectively (Table 2, Figure 1).

P15 gene mutation in rat peripheral blood cells

In a total of 25 peripheral blood samples in osteosarcoma rats, 18 of them (72%) showed mutation in the 2nd exon of P15 gene, while control rats had normal gene isoforms (Table 3, Figure 2).

In examining rats from different time points, one can discover increased mutation rats with elongated time. Further studies also revealed significant correlation between P15 gene mutation and occurrence of osteosarcoma ($r=0.998$, $p<0.05$).

Discussion

Due to its unfavorable prognosis, early diagnosis and treatment is of critical importance for preventing metastasis of osteosarcoma lesions. The clinical features of osteosarcoma mainly include bone pain, hypercalcemia, and osteolysis metastasis [13]. The complication of other organ/tissues, such as the lung, may indicate the metastasis of tumors [14]. The proliferation of primary tumor lesions causes the detachment of tumor cells, which penetrate vessel walls to enter the general lymph or blood circulation system for the invasion of distal tissues, where tumor “seeds” colonize new generations of mitosis [15]. Investigation of the mechanisms underlying the progression and metastasis of osteosarcoma is a popular research topic. Recent studies revealed complicated genetic processes regulating the tumor metastasis [16], as a “hot-spot” located in chromosome 9p21-22 region affects gene fragment loss or transcriptional abnormalities in various malignant tumors [17–19]. P15 gene, as a representative gene in this region, has been shown to have mutants and expression down-regulation in kidney and bladder cancer. In approximately 23% of cancer cells of renal and bladder cancer, the expression of P15 gene is deficient. It has been indicated that single-base mutation occurs in 67, 119, and 135 codons of p15 gene [20]. Due to the methylation of P15 gene, hematopoietic progenitor cells lose the regulation of TGF- β -mediated growth inhibition, which in turn increased the incidence of malignant bone tumors [21]. The growth and metastasis of osteosarcoma have raised wide concern. Recent evidence suggests the complexity of the abnormal regulation of P15 gene involved in bone tumor metastasis. However, the relationship between P15 gene and lung metastasis of osteosarcoma remains to be determined.

This study utilized UMR-106 cell line, which is a classical osteosarcoma cell line induced by radioactive phosphorous isotope (32-P), to generate an osteosarcoma rat model by subcutaneous

injection. The observation of tumor size and pulmonary tissue damage, along with P15 gene expression at different time points after the injection, showed normal tissue structures and almost no tumor cells in the control group. After the inoculation, the overall survival rate of rats was 83.3%, in which about 48% of cases had pulmonary metastasis, suggesting the effectiveness and usefulness of this model. The tumor cell expression maintained at minimal level with lower mutation rate of P15 gene at 1 week after the inoculation. At 2–6 weeks, however, abnormal tumor-like structures began to occur in the pulmonary tissues in the model group, along with elevated P15 gene mutation rates over time. The tumor-positive cell percentage in pulmonary tissues increased from 10% to more than 72% at the final time point (6 weeks), suggesting the occurrence of lung metastasis, as consistent with previous reports [21]. Other studies demonstrated the suppressed incidence of esophagus cancer and pharynx squamous carcinoma by the inhibition of P15 gene methylation [22]. Furthermore, P15 expression level was higher in tongue squamous carcinoma without lymph node metastasis, compared to those patients with metastasis, who also had unfavorable prognosis [23]. All these studies point to the importance of P15 gene in inhibiting tumor growth and invasion, both of which are consistent with our results in osteosarcoma.

References:

- Zhang L, Lyer AK, Yang X et al: Polymeric nanoparticle-based delivery of microRNA-199a-3p inhibits proliferation and growth of osteosarcoma cells. *Int J Nanomedicine*, 2015; 10: 2913–24
- Gao F, Tian J, Liu XD et al: MicroRNA-145 expression in the plasma of patients with benign and malignant bone tumors and its effects on osteosarcoma cell proliferation and migration. *Panminerva Med*, 2015 [Epub ahead of print]
- Lu DF, Wang YS, Li C et al: Actinomycin D inhibits cell proliferations and promotes apoptosis in osteosarcoma cells. *Int J Clin Exp Med*, 2015; 8(2): 1904–11
- Hu Y, Bobb D, He J et al: The HSP90 inhibitor alvespimycin enhances the potency of telomerase inhibition by imetelstat in human osteosarcoma. *Cancer Biol Ther*, 2015; 16(6): 949–57
- Liu S, Wang X, Zhao Q et al: Senescence of human skin-derived precursors regulated by Akt-FOXO3-p27/p15 signaling. *Cell Mol Life Sci*, 2015; 72(15): 2949–60
- Ma D, Fang Q, Wang P et al: Downregulation of HO-1 promoted apoptosis induced by decitabine via increasing p15INK4B promoter demethylation in myelodysplastic syndrome. *Gene Ther*, 2015; 22(4): 287–96
- Magalhaes M, Oliveira PD, Bittencourt AL, Farre L: Point mutations in TP53 but not in p15 and p16 genes represent poor prognosis factors in acute adult T cell leukemia/lymphoma. *Leuk Lymphoma*, 2015 [Epub ahead of print]
- Tian X, Azpuruja J, Ke Z et al: INK4 locus of the tumor-resistant rodent, the naked mole rat, expresses a functional p15/p16 hybrid isoform. *Proc Natl Acad Sci USA*, 2015; 112(4): 1053–58
- Piccione M, Salzano E, Vecchio D et al: 4p16.1-p15.31 duplication and 4p terminal deletion in a 3-years old Chinese girl: Array-CGH, genotype-phenotype and neurological characterization. *Eur J Paediatr Neurol*, 2015; 19(4): 477–81
- Kong R, Zhang EB, Yin DD et al: Long noncoding RNA PVT1 indicates a poor prognosis of gastric cancer and promotes cell proliferation through epigenetically regulating p15 and p16. *Mol Cancer*, 2015; 14(1): 82
- Wei R, Ma X, Wang G et al: Synergistic inhibition of avian leukosis virus subgroup J replication by miRNA-embedded siRNA interference of double-target. *Virology*, 2015; 12(1): 45
- London CA, Gardner HL, Mathie T et al: Impact of toceranib/piroxicam/cyclophosphamide maintenance therapy on outcome of dogs with appendicular osteosarcoma following amputation and carboplatin chemotherapy: A multi-institutional study. *PLoS One*, 2015; 10(4): e0124889
- De Biasio A, de Opakua AI, Mortuza GB et al: Structure of p15(PAF)-PCNA complex and implications for clamp sliding during DNA replication and repair. *Nat Commun*, 2015; 6: 6439
- Kato M, Uemura Y, Sato K et al: Spontaneous remission in a patient with follicular lymphoma carrying T cell-rich neoplastic follicles and a new complex variant translocation of t(14;18): t(5;14;18)(p15;q32;q21.3). *Leuk Lymphoma*, 2015; 56(7): 2187–89
- Balla P, Maros ME, Barna G et al: Prognostic impact of reduced connexin43 expression and gap junction coupling of neoplastic stromal cells in giant cell tumor of bone. *PLoS One*, 2015; 10(5): p. e0125316
- Baker EK, Taylor S, Gupte A et al: BET inhibitors induce apoptosis through a MYC independent mechanism and synergise with CDK inhibitors to kill osteosarcoma cells. *Sci Rep*, 2015; 5: 10120
- Evangelisti C, de Biase D, Kurelac I et al: A mutation screening of oncogenes, tumor suppressor gene TP53 and nuclear encoded mitochondrial complex I genes in oncogenic thyroid tumors. *BMC Cancer*, 2015; 15: 157
- Turner SM, Johnson SM: Abrupt changes in pentobarbital sensitivity in pre-Bötzinger complex region, hypoglossal motor nucleus, nucleus tractus solitarius, and cortex during rat transitional period (P10-P15). *Respir Physiol Neurobiol*, 2015; 207: 61–71

Conclusions

Our results indicate the close correlation between P15 gene mutation and growth of osteosarcoma, and the potentially direct involvement of P15 gene in pulmonary metastasis. Our results suggest the potency of P15 mutant genes as a novel biological marker in early diagnosis of osteosarcoma in clinics, although its detailed molecular mechanism in progression and pulmonary metastasis require further study. Molecular biology research is still required to elucidate the mechanism of mutation location of P15 gene, as well as its role in the metastasis of osteosarcoma to the lung.

19. Kuhar U, Malovrh T: High genetic diversity of equine infectious anaemia virus strains from Slovenia revealed upon phylogenetic analysis of the p15 gag gene region. *Equine Vet J*, 2014 [Epub ahead of print]
20. De Braekeleer M, Guéganic N, Tous C et al: Breakpoint heterogeneity in (2;3)(p15-23;q26) translocations involving EVI1 in myeloid hemopathies. *Blood Cells Mol Dis*, 2015; 54(2): 160–63
21. Miyoshi Y, Noguchi K, Yanagisawa M et al: Nomogram for overall survival of Japanese patients with bone-metastatic prostate cancer. *BMC Cancer*, 2015; 15(1): 338
22. Yang CC, Huang EY, Li HC et al: Nuclear export of human hepatitis B virus core protein and pregenomic RNA depends on the cellular NXF1-p15 machinery. *PLoS One*, 2014; 9(10): e106683
23. Lazarczyk E, Drozniewska M, Pasinska M et al: Complex balanced chromosomal translocation t(2;5;13) (p21;p15;q22) in a woman with four reproductive failures. *Mol Cytogenet*, 2014; 7(1): 83
24. Ciuladaite Z, Preiksaitiene E, Utkus A, Kučinskas V: Relatives with opposite chromosome constitutions, rec(10)dup(10p)inv(10)(p15.1q26.12) and rec(10)dup(10q)inv(10)(p15.1q26.12), due to a familial pericentric inversion. *Cytogenet Genome Res*, 2014; 144(2): 109–13
25. Pala HG, Artunc-Ulkumen B, Uyar Y et al: *De novo* reciprocal translocation t(5;11)(q22;p15) associated with hydrops fetalis (reciprocal translocation and hydrops fetalis). *Fetal Pediatr Pathol*, 2015; 34(1): 44–48